

The Barrel DIRC of the $\bar{P}ANDA$ Experiment

C. Schwarz^a, D. Bettoni^b, D. Branford^c, V. Carassiti^b, A. Cecchi^b, V. Kh. Dodokhof^d
M. Düren^e, K. Föhl^c, R. Hohler^a, R. Kaiser^g, A. Lehmann^f, D. Lehmann^a, H. Marton^h,
K. Peters^a, G. Schepers^a, L. Schmitt^a, P. Schönmeier^e, B. Seitz^g, C. Sfienti^a, A. Teufel^f,
and A.S. Vodopianov^d

^a*Gesellschaft für Schwerionenforschung mbH, Planckstraße 1, D-64291 Darmstadt, Germany*

^b*INFN Ferrara, Via Paradiso 12, I-44100 Ferrara, Italy*

^c*School of Physics, University of Edinburgh, Edinburgh EH9 3JZ, United Kingdom*

^d*Laboratory of High Energies, Joint Institute for Nuclear Research, 141980 Dubna, Russia*

^e*II. Physikalisches Institut, University of Gießen, D-35392 Gießen, Germany*

^f*Physikalisches Institut Abteilung IV, University of Erlangen-Nürnberg, D-91058 Erlangen, Germany*

^g*Department of Physics & Astronomy, Kelvin Building, University of Glasgow, Glasgow G12 8QQ, United Kingdom*

^h*Stefan Meyer Institut für subatomare Physik, Austrian Academy of Sciences, A-1090 Vienna, Austria*

Abstract

Cooled antiproton beams of unprecedented intensities in the energy range of 1-15 GeV/c will be used at the $\bar{P}ANDA$ experiment at FAIR to perform high precision experiments in the charmed quark sector. The charged particle identification in the barrel region needs a thin detector operating in a strong magnetic field. Both requirements can be met by a Cherenkov detector using the DIRC principle. Combining the time of arrival of the photons with their spatial image determines not only the particles velocity, but also the wavelength of the photons. Therefore, dispersion correction at the lower and upper detection thresholds is possible. Special care has to be taken to couple the photon detector to the barrel radiator bars.

Key words: Particle identification, Cherenkov counter, ring imaging

PACS: 29.40.Ka

1. Introduction

Particle identification (PID) for hadrons and leptons over a large range of solid angle and momenta is an essential requirement for meeting the physics objectives at the $\bar{P}ANDA$ detector (1). The charged PID in the barrel section of the target spectrometer has to work in the strong magnetic field of $B \approx 2$ T within the solenoid. Additionally, it cannot take too much radial space, since it is surrounded by an electromagnetic calorimeter. The detection of momenta

up to several GeV/c can be performed by the Detection of Internally Reflected Cherenkov (DIRC) light as realized in the BaBar detector (2)(3)(4). Particles in the angular range of $22^\circ - 140^\circ$ are relatively slow, so that one can use materials with high refraction indices favoring the internal reflection of photons. The lower momentum threshold of kaons producing Cherenkov light is as low as $p = 460$ MeV/c for an refractive index of $n = 1.47$. The polar angles and energies of kaons from the decay of J/ψ s are shown in Fig. 1. Since $\bar{P}ANDA$ is a fixed-target experiment, the distribution of kaons is forward-peaked and will be detected mainly in the endcap DIRC (6)(7)(8) and the forward part of the bar-

Email address: C.Schwarz@gsi.de (C. Schwarz).

URL: <http://www.gsi-panda.de> (C. Schwarz).

rel DIRC. The barrel DIRC will detect kaons from 22° to approx. 120° due to the kaon threshold for Cherenkov light. A radial space occupancy of 10 cm is foreseen to hold the radiator slabs, the mechanical mount and eventually a thin time of flight barrel.

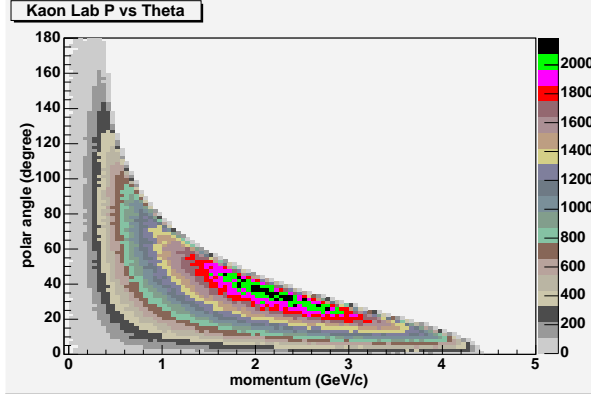


Fig. 1. Radiative decays of resonances in formation experiments like $J/\psi \rightarrow K^+K^-\gamma$ for the search of glue balls (5). The figure shows the polar angle *vs.* momentum distribution of the kaons.

2. The detector

As a first approach a version of the installed BaBar detector scaled down in size was favored. Since the photon detector uses a pin hole focus, the diameter of the photo-multiplier tubes (PMTs)

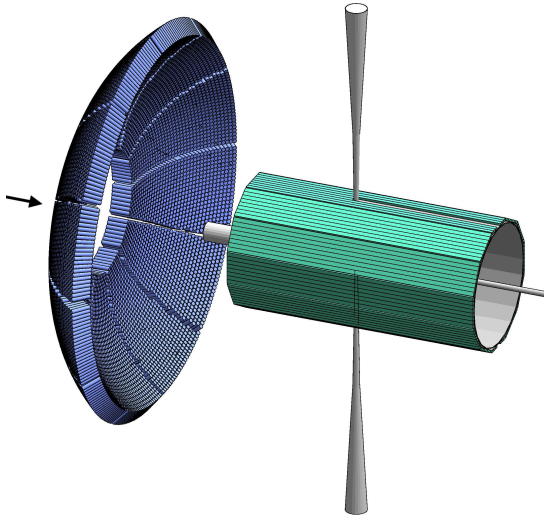


Fig. 2. The $\bar{P}ANDA$ barrel DIRC as a version of the BaBar-DIRC scaled down in size. The diameter of the barrel is 1 m .

has to match the light-exit geometry of the radiator slabs, which is $17 \times 35\text{ mm}^2$. In addition, the distance between PMT and radiator exit must be large compared to the lateral dimensions of the radiator cross section to produce a sharp image. Due to the smaller radius of the $\bar{P}ANDA$ radiator barrel, the number of PMTs is reduced from ≈ 11000 to ≈ 7000 . A sketch of this scaled down detector is shown in Fig. 2. The beam comes from the left as indicated by the arrow. On the right the radiator barrel is crossed vertically by the target pipe of a cluster-jet or a pellet target. Therefore, in the direction forward of the target pipe two radiator slabs are missing, one at top and one at bottom. Centered within the barrel a piece of the beam pipe is visible. In the forward direction the ends of the radiators are covered with a mirror reflecting the Cherenkov light back towards the photon detector. On the left the ≈ 7000 PMTs of the photon detector are shown. The coupling between the end of the radiator slabs, a water box, is not shown. We simulated the response of the DIRC barrel with reaction products coming from $\bar{p} + p \rightarrow J/\psi + \Phi$. The results are shown in Fig. 3. In this figure there is a

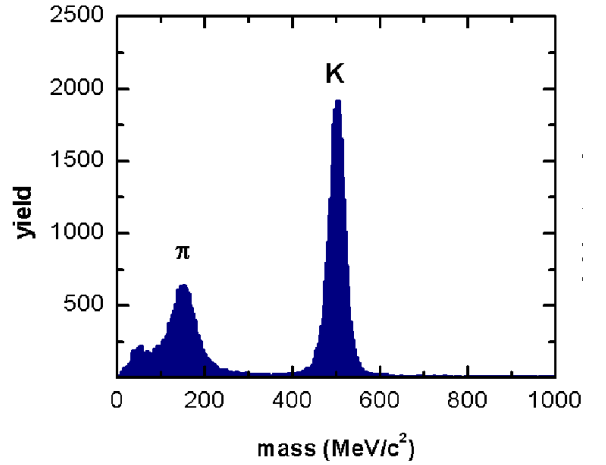


Fig. 3. Reconstructed particle mass from the momentum and the Cherenkov angle information.

well separated peak from kaons and another peak from pions. The efficiency for the DIRC to identify a kaon has been investigated, and it is plotted as a function of momentum (open circles, ordinate scale on the right) in Fig. 4 for kaons in the mass region of $450 - 550\text{ MeV}/c^2$. The corresponding probability that a pion is incorrectly identified as a kaon is presented as the full circles (ordinate scale on the

left) for the same mass region. The loss of efficiency for positive kaon identification at low momenta is caused by failing to produce enough Cherenkov photons. This loss of efficiency can be avoided by operating the detectors in the veto mode, i.e. all low momentum tracks are considered to be kaons except those with Cherenkov signals. The purity of the kaon sample in this mode, however, depends on the detailed composition of the background.

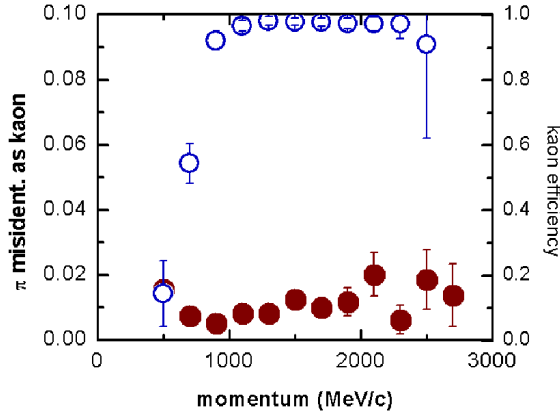


Fig. 4. The probability to misidentify a pion as a kaon as a function of the particle momentum (closed circles) and the efficiency to identify a kaon (open circles).

3. Developments

The high refractive index of the radiator challenges to master the wavelength dependent Cherenkov angles due to chromatic dispersion. This dependency is about 10000 times stronger than in gaseous radiators. It limits the high-momentum resolution, when the particle approaches speed of light, because Cherenkov angles in this regime differ only slightly. Also the resolution at low energy may suffer from strong dispersion since, due to the cosine term of the Cherenkov angle, a small change in the refractive index at the threshold leads to a large angular change. This is seen in Fig. 5 where the image comes from a particle with a velocity just above the threshold $\beta = 0.69c$. The blurred image becomes sharp as one increases the velocity shown in Fig. 6 ($\beta = 0.72c$). The colors, if visible, of the photons in the figures resemble their wavelength. If the time when the charged particle is produced is known and the time of arrival of the photons is measured, the additional information allows to de-

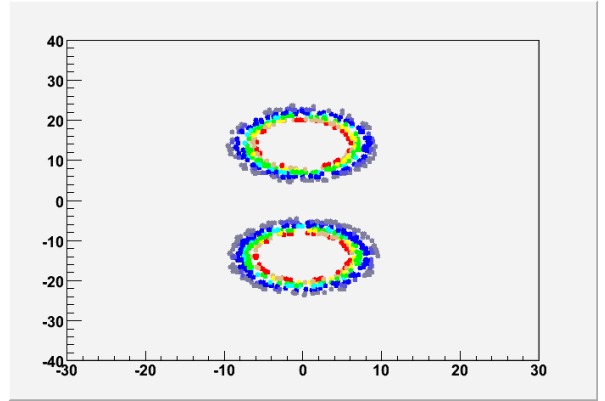


Fig. 5. Spatial image of a particle with speed $\beta = 0.69c$ produced in a fused silica radiator. The doubling of the ring structure comes from top-down reflections within the radiator.

termine the wavelength of the photon and changes the DIRC in a 3D-DIRC with the ability to correct dispersion. The necessary time resolution should be better than $\Delta t = 0.5 ns$ and favors photon detectors like multi-channel-plate PMTs eg. the BURLEPLANACON PMTs (11). Their small pixel size also allow to construct a smaller photon detector. However, since the pixel size does not match the radiators cross section focussing optical elements are needed (9). Using mirrors one encounters problems with split Cherenkov rings from photons hitting two different mirrors. For the photon detector of the barrel shaped structure 12-16 mirrors are needed. The optics of lenses needs a careful design, since refraction works only at optical boundaries with sufficient refractive power, e.g. fused silica-air, without creating too much dispersion. A possible setup foresees fused silica lenses at the radiator ends which focus the photons on a plane. After a small air gap

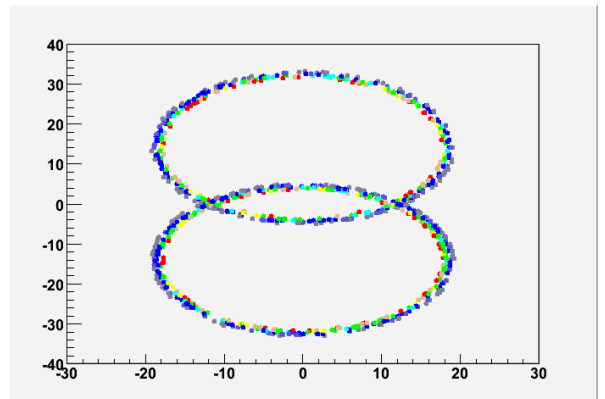


Fig. 6. Spatial image of a particle with speed $\beta = 0.72c$.

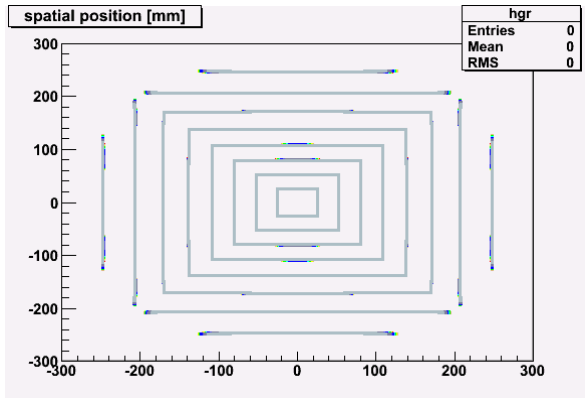


Fig. 7. Spatial image of rectangular structures to identify image distortions. The distance between the different structures along the X and Y axes are 5° degrees apart.

of ca. 1 mm a flat fused silica window, which limits a photon detector vessel filled with a medium with similar refractive index like oil, prevents cushion shaped image distortions. These distortions are of the same kind as the view of a fish in water observing objects at land, in air. The simulation of such a lens is shown in Fig. 7 for a photon detection plane 25 cm behind the fused silica window. The photons were generated such to produce rectangular structures to identify image distortions. The angular distance between the different structures along the X and Y axes is 5° degrees. For larger angles the corners of the rectangular structures are not visible anymore. Here, the photons are reflected out in the air gap. These large angle photons are subject of larger image distortion and would deteriorate the Cherenkov image. A detailed view of the outer lines in Fig. 7 is shown in Fig. 8 and makes the image distortion visible. The dimensions of such a photon detector are in the order of 25 cm . It is conceivable to integrate it within the solenoid yoke of the $\bar{P}ANDA$ detector, since channel plate PMTs depending on the channel diameter are able to work in a strong magnetic field (10).

4. Conclusions

While a DIRC as it exists at BaBar/SLAC would fulfill the charged PID requirements of the $\bar{P}ANDA$ detector, we initiate the development of a smaller photon detector easier to integrate within the complete detector setup. Using fast detectors with time resolution better than 0.5 ns allows to employ the timing information for dispersion correction, not only for high momentum particles but

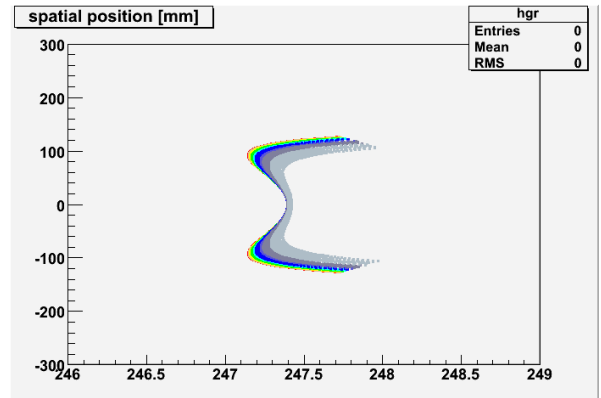


Fig. 8. Detailed view of Fig. 7. Since the photons are emitted under distinct Cherenkov angles, the observed dispersion comes solely from the air gap.

also for particles just above the Cherenkov threshold. We favor a photon detector coupled with a small air gap to the radiator slabs with focussing lenses. This reduces image distortions, sorts out large angle photons deteriorating the Cherenkov image, and allow also for a more simple integration of the photon detector in the complete setup: Due to the air gap the photon detector can be easily removed and reconnected. Efforts are taken to produce a small-scale prototype.

5. Acknowledgements

This work is supported by EU FP6 grant, contract number 515873, DIRACsecondary-Beams.

References

- [1] M. Kotulla et al., “Strong interaction studies with antiprotons. Letter of intent for PANDA
- [2] R. Aleksan et al., Nucl. Inst. Meth. **A397**, 261 (1997).
- [3] I. Adam et al., SLAC-PUB-10516.
- [4] G. Vasileiadis, Nucl. Instrum. Meth. **A384**, 175 (1996).
- [5] M. S. Chanowitz and S. R. Sharpe, Phys. Lett. **B132**, 413 (1983).
- [6] K. Föhl et al., these proceedings
- [7] P. Schönmeier et al., these proceedings
- [8] M. Hoek et al., these proceedings
- [9] J. Vavra et al., SLAC preprint SLAC-PUB-12803.
- [10] A. Lehmann et al., these proceedings
- [11] <http://www.burle.com/>.